THE AMERICAN SOCIETY OF MECHANICAL ENGINEERS
345 E. 47 St., New York, N.Y. 10017

85-IGT-9

The Development of a Second-Generation of Controlled Diffusion Airfoils for Multistage Compressors

R. F. BEHLKE
Project Engineer
Commercial Engineering
Pratt & Whitney, United Technologies Corporation
East Hartford, Connecticut

ABSTRACT

The evolution of Controlled Diffusion Airfoils[1] is traced from inception of the theoretical design model to demonstration of significant performance gains at engine operating conditions in a multistage compressor rig. The proven aerodynamic benefits and versatility of first-generation Controlled Diffusion Airfoil blade elements are extended to the endwall flow region using an Integrated Core/Endwall Vortex design model to produce a new full span optimized second-generation Controlled Diffusion design. Highlighted are the essential roles of extensive cascade, low speed, large scale and high Mach number compressor rig testing in developing and substantiating the second generation Controlled Diffusion technology resulting in a 1.5% increase in efficiency and 30% increase in surge-free operation relative to first-generation Controlled Diffusion Airfoils.

INTRODUCTION

The demand for lower fuel consumption and reduced cost of modern gas turbine engines has led to a requirement for both increased efficiency and higher aerodynamic loading capability in compressors. The application of the first generation of non-standard airfoils, designated "Controlled Diffusion Airfoils"[1], in the seventies was a major contribution to demonstrated increases in compressor performance (Figure 1). Commercial engine compressors with Controlled Diffusion Airfoils were improved by 2% in polytropic efficiency and 60% in pressure rise per airfoil by the early eighties. The NASA/Pratt & Whitney Energy Efficient Engine compressor demonstrated the ability to push the improvement in pressure rise per airfoil to 150% of the standard airfoil technology of the seventies while improving efficiency by 1%. Controlled Diffusion Airfoil (CDA) technology produced benefits beyond the flowpath, rotational speed, and configuration changes by increasing both efficiency and airfoil pressure loading; it was instrumental in bringing the compressor state-of-the-art performance above 90% polytropic efficiency. Controlled Diffusion Airfoil technology also produced significant reductions in the airfoil count of the PW2037 and PW4000 commercial engines. As this paper will show, further gains in efficiency and surge margin are attainable with a new generation of Controlled Diffusion Airfoils.

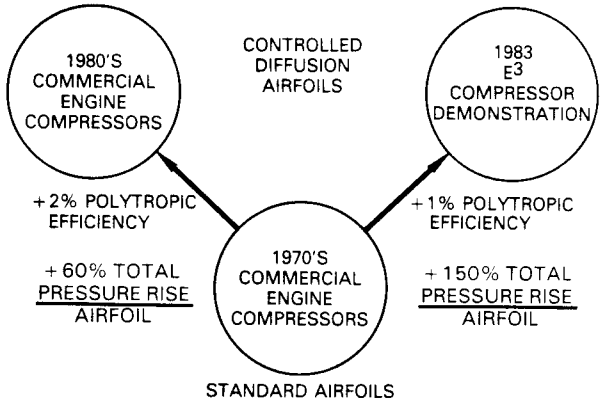

Fig. 1 1st Generation Controlled Diffusion Airfoils Efficiency and Loading Contributions

These airfoil technical advances were built on the foundation of a modern two dimensional compressible potential flow code combined with improved boundary layer codes providing the capability to design sections which minimize boundary layer growth and prevent boundary layer separation. When applied to the multistage core compressor environment, however, the ability of these modern airfoil sections to meet their peak aerodynamic potential is limited by the three dimensional effects imposed by the endwall environment. Secondary flow patterns are caused by 1) cross channel, pressure-gradient induced vortices, 2)

[1] "Controlled Diffusion" is the trade name given by Pratt & Whitney to a simplified procedure for specifying the geometry of high performance, custom designed airfoil sections disclosed under U.S. Patent # 4,431,376

Presented at the 1985 Beijing International Gas Turbine Symposium and Exposition
Beijing, People's Republic of China — September 1-7, 1985

tip clearance loss in rotors, 3) cavity loss in stators, and 4) general endwall friction (Ref. 1). These patterns modify the flowfield so drastically that their effects must be accurately modelled and reflected in the design geometry to achieve peak performance. This is especially true in the middle and rear stages of multistage compressors where higher hub/tip ratios, lower aspect ratio and a highly developed endwall boundary layer produce endwall efficiency penalties on the order of 5.0 percentage points. That is, about 50% of the total inefficiency is caused by endwall effects.

Further advances in the state-of-the-art of multistage compressor design require a design approach that extends the refined CDA blading philosophy into the endwall region for optimized full span performance. This paper traces the development of such a design system and its use in originating a new family of advanced compressor airfoils--second-generation Controlled Diffusion Airfoils developed for future models of modern engines. The evolution of second-generation Controlled Diffusion Airfoils (CDA-II) is followed from analytical model to performance demonstration to show the critical roles and relationship of cascade, large scale, and low Mach number compressor rigs in the development of this new technology.

DESIGN AND DEVELOPMENT APPROACH

The design and development of high speed multistage compressors is one of the most demanding technical challenges in engineering today. It is a multi-dimensional problem. A complex three dimensional flowfield exists in each blade row. The multiplicity of blade rows, their aerodynamic interaction and the desire to have all rows reach peak performance simultaneously are added dimensions. The challenge of finding and developing new technology in this atmosphere requires a sophisticated approach which accurately models the physics of these complex aerodynamic interactions.

The first-generation CDA design approach concentrated on the optimization of airfoil sections in the core, or the region of the span little affected by wall effects, using extensive cascade testing to substantiate modelling of the blade-to-blade potential flowfield and boundary layer. The endwall regions whose extent and aerodynamics were defined by simple empirical correlations were treated as boundary conditions to the core. Endwall blading was treated as an extension of the core blading modified only in metal angle based on a boundary layer approximation. The substantiation of this first-generation approach occurred in full multistage rigs in the NASA Energy Efficient Engine program and in rigs and engines of commercial engine programs.

The design-development approach presented here for second-generation Controlled Diffusion Airfoils combines an aerodynamic model with cascade, low and high Mach number rig testing to extend the proven benefits and versatility of Controlled Diffusion blade elements into the endwall region. The elements of this second-generation CDA approach are presented in flow chart form in Figure 2 to show their relationship among themselves and to the first generation CDA design foundation on which this approach is built. The core and endwall CDA blading elements utilizing both profile shape and angle interact through the integrated flowfield model to optimize full span performance. The cascade, large scale, low and high Mach number compressor rigs provide detailed flowfield and blade element data feedback to develop and substantiate aerodynamic models for wall friction, tip clearance and cavity effects. These rigs form a comprehensively instrumented and controlled environment, which provides great accuracy in isolating and understanding aerodynamic effects. They are building blocks in the formulation and substantiation of the model leading to overall verification and feedback in high Mach number rig testing. The High Mach Number Closed Loop Compressor Test facility reproduces the engine environment to provide final verification that the technology is immediately usable under engine conditions without the necessity of transformation for Mach number and Reynolds number effects. The formulation of each of these elements and their role in the development and successful demonstration of the second-generation controlled diffusion design is discussed below.

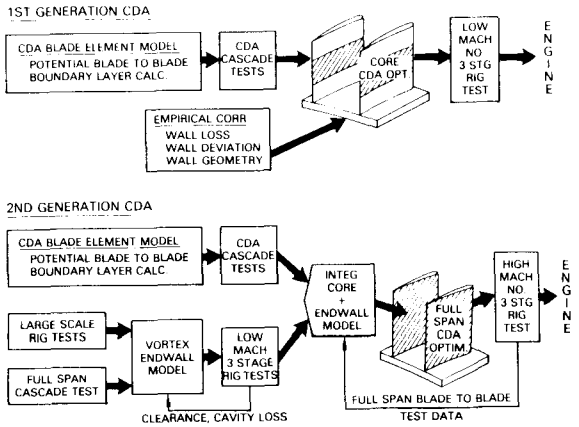

Fig. 2 2nd Generation CDA Design-Development Approach Extends CDA Technology to the Endwalls

BASIC CONTROLLED DIFFUSION AIRFOIL FOUNDATION

The success of first-generation Controlled Diffusion Airfoils in producing increased efficiency and loading capability of subsonic and transonic airfoils in modern compressors resulted from extensive theoretical analysis and cascade testing extending back to 1974. The significant milestones in the development of this technology are presented in detail by Weingold and Hobbs in reference 2. The Controlled Diffusion Airfoil design criteria resulting from this technology are illustrated in Figure 3. The major features of these criteria are 1) continuous suction surface Mach number acceleration to boundary layer transition, 2) peak Mach number less than 1.3 and 3) diffusion rate controlled to prevent separation and minimize skin friction.

Cascade test results presented in reference 2 confirmed that airfoil sections designed to these criteria could operate at higher Mach numbers with less loss penalty than standard airfoils and with up to 25% greater incidence range at a given loss. These benefits have undoubtedly contributed greatly to their success in multistage compressors where matching of the many airfoil rows, stagewise and spanwise, is a major problem. The cascade testing of these initial CDA sections also provided feedback on the accuracy of the aero codes and design criteria.

An example of the agreement of design code surface Mach number prediction versus Mach number derived from test surface static pressure measurements is given in Figure 4; the data show excellent agreement for a highly loaded 1.0 solidity section tested in both a cascade tunnel and at 50% span of a single stage stator. Figure 4 also reveals in its smooth monotonic closure of suction and pressure surface Mach numbers at the trailing edge that the design goal was met: elimination of separation by control of diffusion rate through scheduling of profile thickness and angle. The second generation CDA approach retains this basic CDA foundation but adapts it to the endwall environment.

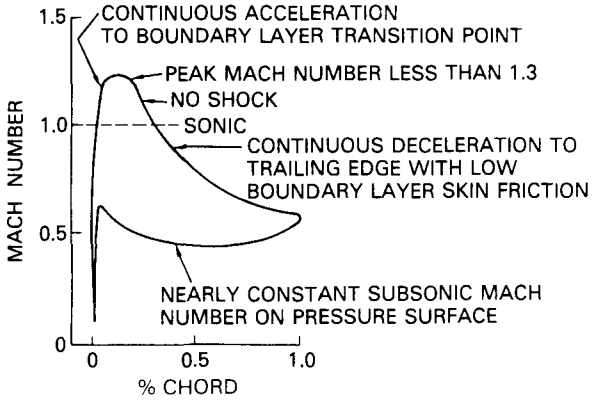

Fig. 3 1st Generation CDA Design Criteria Are Adapted to the Endwalls in the 2nd Generation Approach

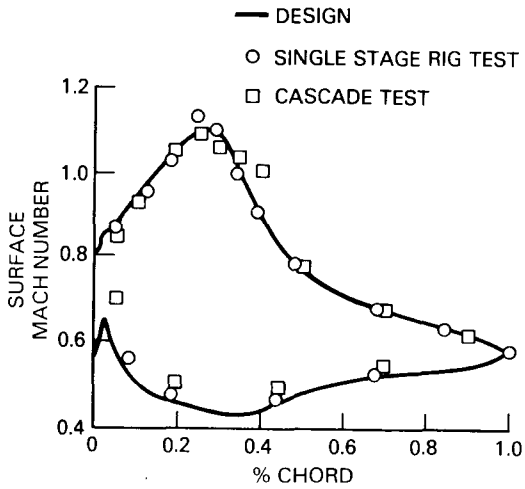

Fig. 4 Cascade and Single Stage Rig Airfoil Surface Static Pressure Measurements Verify the CDA Blade Element Design System

EXTENSION OF BASIC CDA PHILOSOPHY TO THE ENDWALLS

Formulation of the Integrated Core/Endwall Aerodynamic Model

The foundation of the second-generation CDA design is the formulation of an analytical design model which accurately represents the physics of the multi-dimensional flowfield and its interaction with airfoil blade element geometry. The major elements of this integrated core/endwall aerodynamic model are presented in Figure 5. This design model combines a two-dimensional, potential blade element solution with compressible boundary layer calculation from wall to wall; subroutines calculate loss and deviation when the airfoil boundary layer is separated, as often occurs near walls. Superimposed on this base are vortices which wrap up endwall loss sources including wall friction, tip clearance, shroud cavity and undecayed upstream effects. The resultant spanwise loss and turning distributions are fed into an axisymmetric streamline program which integrates their effect on the flow field through radial equilibrium and continuity solutions.

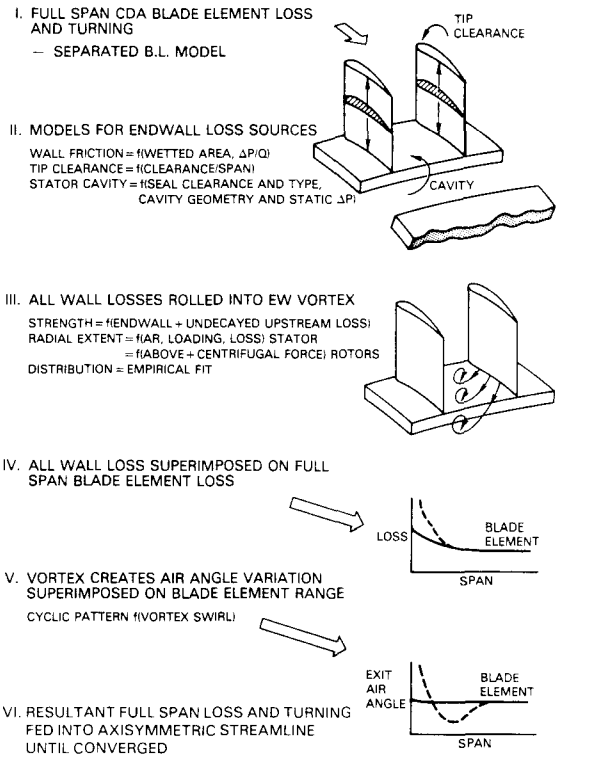

Fig. 5 Integrated Core/Endwall Aerodynamic Model Used in the 2nd Generation CDA Designs

The interaction of the CDA-designed endwall airfoil sections with the aerodynamics imposed by the endwall flowfield provide the necessary ingredients for optimizing the endwall airfoil shapes and inlet and exit angles. This provides design capability to reduce endwall loss and increase endwall loading capability for increased surge margin. An equally important feature of this system is the feedback of loss and turning from the CDA endwall airfoil sections to the endwall flowfield aerodynamic model to more accurately set the endwall blockage and boundary conditions on the two dimensional core. This improved evaluation of interaction of core and endwall permits optimization of each for maximum overall performance. A more complete discussion of the formulation of this design system and its substantiation by cascade, large scale, low and high Mach number rig testing follows.

Substantiation of the Vortex Aerodynamic Model in Stators

It has been shown in Figure 4 that the CDA blade element model is effective in representing unseparated two-dimensional cascade and stator core

sections. The extension of CDA blade elements to the endwalls, however, requires an analytical model capable of handling severely stalled and often separated sections. Accurate modeling of separated airfoil loss and turning is needed to provide a vehicle for determining the best section shape and angle for optimum endwall performance. A separated loss and turning model was developed for second-generation Controlled Diffusion Airfoils using two-dimensional cascade test data and added to the basic boundary layer calculation. This model relates the loss and turning of a separated cascade to the Mach number and boundary layer properties at the calculated point of separation from the potential flow/boundary layer solution. Loss is calculated for a mixing process at the separated Mach number; deviation has been modeled as a function of separation point, potential unseparated turning and cascade geometry.

A basic source of endwall loss in stators and all configurations is frictional drag. In the Integrated Core/Endwall Aero Model, friction is considered to be due to boundary layer growth resulting from the pressure gradient impressed on the endwall by the airfoil cascade. It is modeled as a function of loading (Δ P/Q), Reynolds number, and cascade geometry, and integrated from blade-to-blade along the wall with analytical modifications for airfoil boundary layer separation and removal of fluid by the vortex. This is one of the loss sources wrapped up into the endwall vortex.

The accuracy of the model in predicting the full span loss and turning of a stator is shown in Figures 6a and 6b for a highly loaded 65/CA cascade in which total pressure and angle measurements were taken from wall-to-wall. The blade element and friction elements of the model calculated loss are shown at the top of Figure 6a while the blade element and endwall vortex ingredients of turning are presented below. The presence of underturning due to the vortex is shown in both the model-prediction and the data. The ability of the blade element model to predict pressure rise of both unseparated core sections and separated endwall sections is shown in Figure 6b.

The strength of the endwall vortex in stators is increased beyond that of the above example by virtue of shroud cavity or cantilevered stator clearance loss. The flowfield modeling assumes that these wall losses, tip clearance and stator cavity losses are rolled up into a vortex which cleans the endwall region of low momentum fluid. These losses are redistributed in the vortex and are seen as an unrecoverable solid body swirl velocity superimposed on the freestream velocity. The direction and magnitude of the vortex varies according to the driving source. A tip clearance vortex is opposite in direction to the tip wall vortex with the stronger of the two setting the resultant direction. Cantilevered stator root losses are derived from a correlation of loss versus tip clearance/span while stator cavity losses have been modeled as a function of pressure rise, seal tip clearance and cavity geometry. Both of these correlations were based on low speed, three stage compressor rig testing to relate performance changes to specific geometric variations. The pressure gradient of a shrouded stator root produces a vortex opposite in rotation to that of a cantilevered stator which is driven by the tip clearance flow.

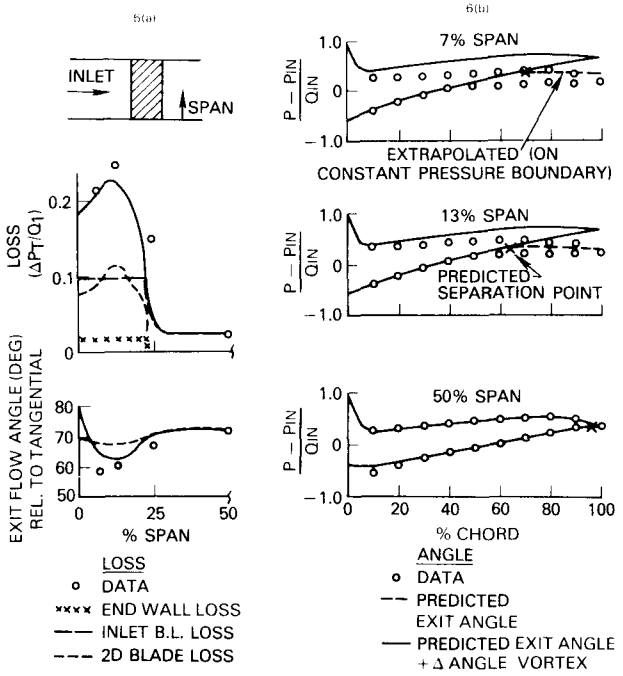

Fig. 6 Aerodynamic Model Matches Test Airfoil Surface Static Pressure, Loss, and Turning at Midstream and Endwalls of a 65/CA Stator Cascade with 40 Degrees of Camber

These modelling concepts were graphically illustrated by back-to-back cantilevered and shrouded stator tests in the low Mach number three-stage rig shown in Figure 7. Cantilevered and shrouded inner wall angle measurements underturned and overturned respectively in opposite directions, and the outer wall showed overturning for both stator constructions. The physics of the vortex model reflect the spanwise turning effects due to stator construction, as shown in this data.

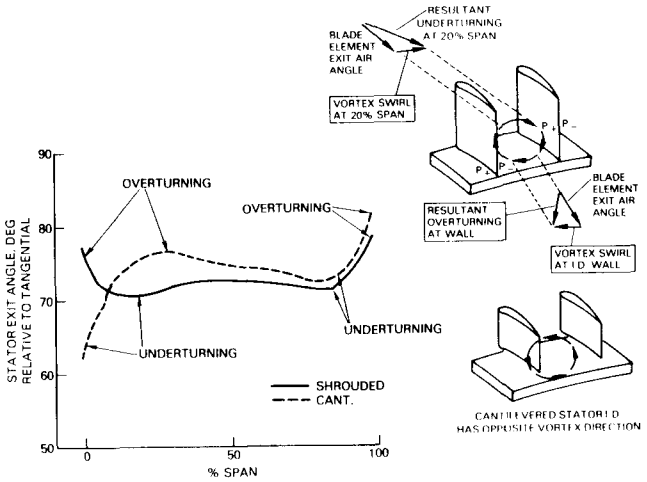

Fig. 7 Low Mach Number, 3 Stage Rig Testing Shows the Influence of Stator Construction on Vortex-Induced Endwall Overturning and Underturning

Substantiation of Vortex Model in Rotors

Vortex strength and radial extent in rotors are driven by the same physical forces as in stators, but one must consider the addition of centrifugal force in the determination of radial extent. Rotor tips are modeled similar to the free ends of cantilevered stators where the sign of the clearance flow vortex is opposite to that of the solid wall. Rotor roots are geometrically similar to stator outer shrouds, but one must add a centrifugal stretching effect caused by the dragging of endwall particles up to wheel speed (U) by wall friction and the resultant lack of equilibrium due to high centrifugal force and low axial momentum. Rotor tips are not assumed to experience these forces, since the outer wall is not rotating and acts as a constraint to radial flow. In addition, tip leakage flow acts against swirl causing a reduction in centrifugal force.

Modeling of the rotor root vortex stretching concept was substantiated with the use of a large scale rotating compressor rig. This rig employs its five foot diameter and slow rotational speed to make detailed surveys of exit total pressure and angle in the rotating reference frame of the rotor. Coupled with rotor surface static pressure measurements and flow visualization techniques, these surveys provided the ability to assess the location and strength of the vortex and determine its impact on blade element performance thus contributing to two parts of the model. This rig has been run in both isolated rotor and two stage versions. Test results for a 6 inch chord, aspect ratio of 1.0 isolated rotor with hub/tip of 0.85 (Refs. 3 and 4) were used in the development of the rotor model. Figure 8 compares the model-predicted blade element pressure coefficient with test-measured values on the rotor pressure and suction surfaces of this rig. Predicted values are in close agreement with suction surface measured values across most of the span; this provides an accurate basis for calculating loss and turning. The more stalled-looking test distributions on the root sections are not duplicated exactly by the model, but the overall pressure rise is closely matched. The model is calibrated to produce correct overall pressure rise and loss, permitting the optimization of endwall sections.

The lack of a viscous interaction between the potential flow and boundary layer calculations and the circumferential averaging of inlet and exit boundary conditions are compensating approximations in this approach which tend to facilitate the calibration of overall properties. An exact three-dimensional solution with viscous effects would be more desirable, but it would add significant complexity and is beyond current computational capability in multistage compressors. The simplified modeling presented here produces the correct overall result; it will be shown to provide an excellent basis for developing improved endwall performance technology.

A final substantiation of the analytical model using the Large Scale rig data was the comparison of the model's integration of core and endwall loss and turning with measured values. The measured spanwise total pressure loss curve and measured rotor relative exit air angle in Figure 9 agree closely with predicted values. The large tip loss and underturning of this blade reflect its large tip clearance of 2.2% span. It is also evident in the test root loss that centrifugal stretching out of the loss to 50% of span is well represented by the model. Without this centrifugal stretching parameter the predicted endwall loss would have extended only to 25% of span and underestimated the loss at that span.

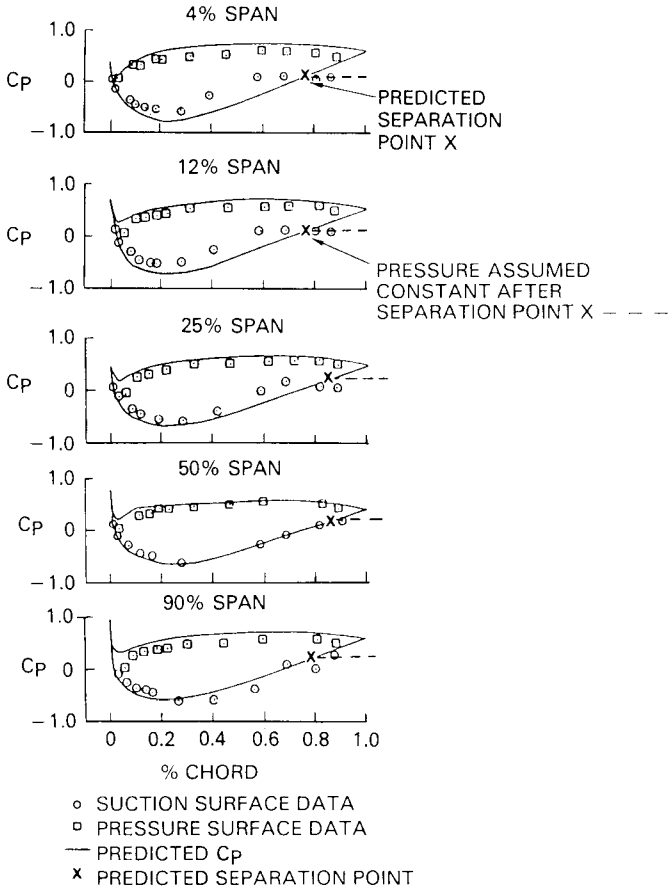

Fig. 8 Surface Static Pressure Measurements in the Rotating Frame of the Large Scale Rig Confirm the Aerodynamic Model to within 4% Span of the Wall

Substantiation of Multistage Effects Using Low Speed Rigs

The previous sections were concerned with the development and substantiation of individual elements of the analytical model which are present in isolated blade rows. This section addresses the need to model differences in the flow field caused by linking these blade rows in a multistage compressor.

The added element occurring in the prediction of multistage performance is the necessity to translate aerodynamic conditions from upstream to downstream blade rows. In this relatively short axial interval, wakes decay, vorticity dissipates, spanwise profiles are mixed, and a change in reference frame occurs. These phenomena are treated in the Integrated Core/Endwall model by two devices: the spanwise profiles and a retained vorticity parameter. Blade row

discharge blade element total pressure, total temperature and angle profiles are transferred at constant angular momentum along streamlines to the downstream row leading-edge. It is assumed that, in the core region of the span, wakes are dissipated before reaching the following rows' leading edge. In the endwall region, however, the upstream vorticity and wakes were found to strengthen the downstream row's vortex based on studies of differences between isolated rotors and several multistage compressors. This incomplete mixing process was found to follow a logarithmic function of axial gap between rows, upstream chord, airfoil circumferential spacing and the strength of the loss source. The analytical model with this downstream decay feature was employed to predict multistage rigs of differing axial gaps, blading geometry and endwall defects to test and develop its predictive capability. Two pairs of these prediction examples will be presented here.

Low Mach number, three-stage rig tests were chosen to illustrate the model's predictive ability for a multistage rig with close axial gapping (16% of chord) and strong endwall effects by virtue of its low aspect ratio (1.0). The low Mach number, three-stage rig has been used to assess a large number of aerodynamic and geometric parameters including flowpath, airfoil tip clearance and cavity variations.

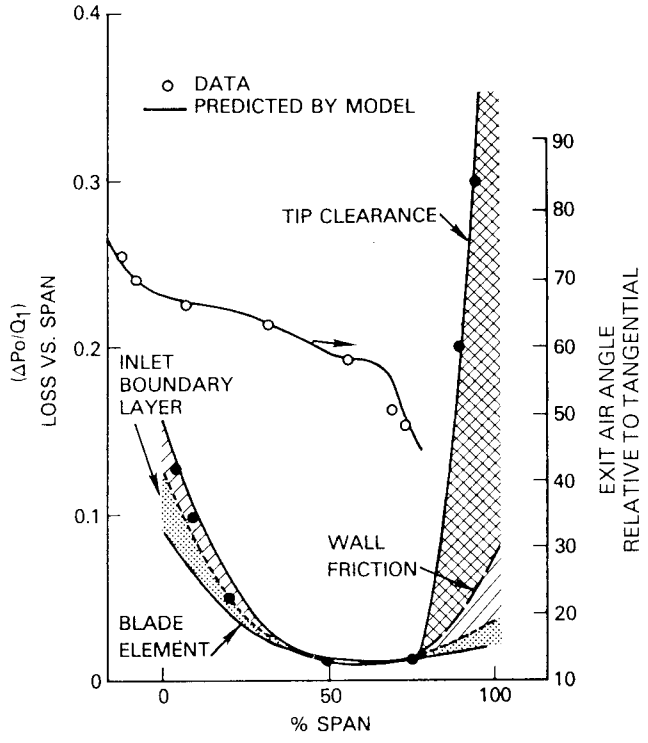

Fig. 9 Large Scale Rig Loss and Angle Measurements Confirmed the Integrated Core/Endwall Model Predictions in the Rotating Frame

The three-stage rig has the capability to independently vary rotor and stator stagger to optimize matching at different loading levels. Leading-edge and overall total pressure and temperature pole rake instrumentation as well as extensive wall static pressure measurements in a controlled environment make this rig a valuable developmental tool. It is employed to assess overall performance and stage matching; more importantly, it is capable of assessing spanwise profile differences as parameters are varied to evaluate endwall health. A comparison of the model-predicted total pressure and total temperature profiles versus test values for the 3rd stator leading edge of a baseline build of this rig in Figure 10 shows good overall agreement in shape. The large pressure defect below 50% span in the test data is also well represented by the model, reflecting a strong vortex due to the low aspect ratio which feeds downstream as a result of the close axial gaps. A test in this same rig of a 5 degree closed restagger of the blading also provided an opportunity to assess the model's ability to predict performance differences due to geometry changes. Comparison of exit spanwise profiles and overall performance for these two rigs to model-predicted values are given in Figure 11. As in the internal leading-edge data comparisons the spanwise character of the profiles is represented closely. The overall performance difference resulting from the increased loading at reduced stagger is also closely predicted.

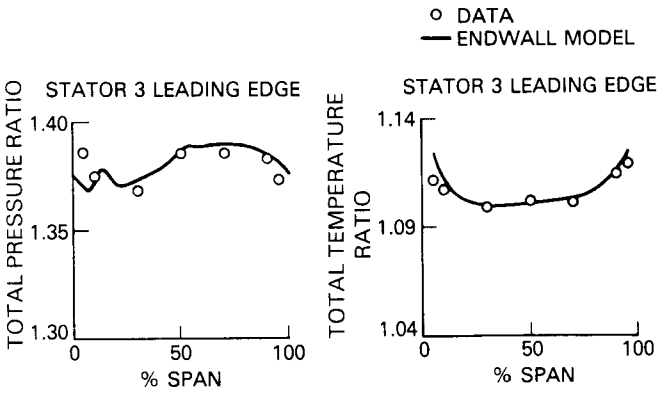

Fig. 10 Integrated Core/Endwall Model Predicts Spanwise Profiles of the Low Mach Number, 3 Stage Rig, Illustrating Its Multistage Capability

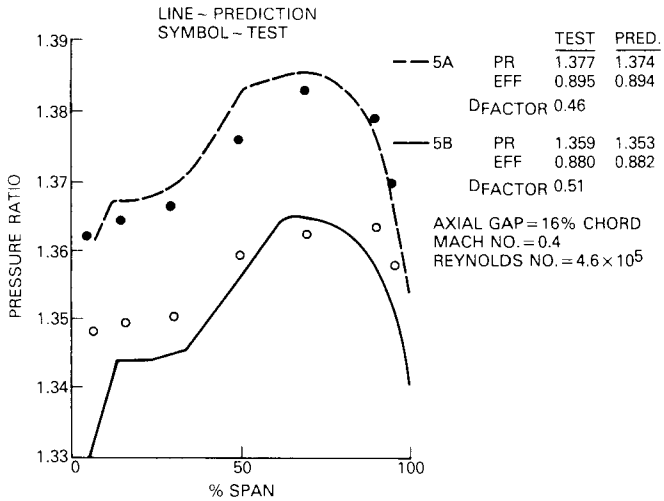

Fig. 11 Integrated Core/Endwall Model Matched Spanwise Profiles and Overall Performance Differences of the Low Mach Number, 3 Stage Rig at Two Loading Levels

Data published in references 5 and 6 by General Electric from a large scale, four-stage rig also provided an opportunity to test the model's ability to predict performance for a more widely spaced (33% chord) and higher aspect ratio (1.2) rig. As might be expected, the endwall pressure fall-off shown in Fig. 12 is not as pronounced as that of the lower aspect ratio more closely spaced three-stage rig previously discussed. The Integrated Core/Endwall model captures the essence of this fuller profile in the comparison in Figure 12, although the innermost pressure reading falls off more than predicted. It is noteworthy that the model predicted the overall test efficiency gain of 0.3% when the stators of this rig were twisted closed at the endwalls by 8.0 degrees. The predicted efficiency gain was primarily within 20% of the endwalls where the twists occurred and where the major differences in test pressure profiles occurred.

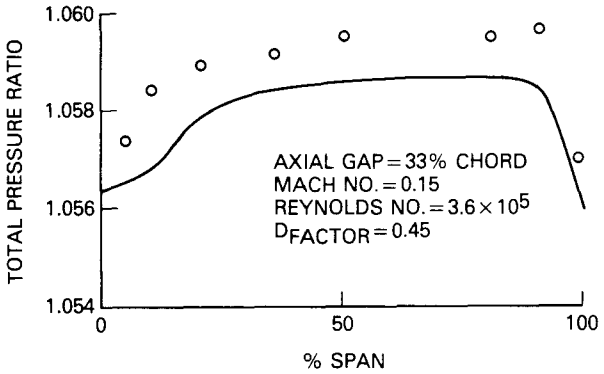

Fig. 12 Aerodynamic Model Matches the Exit Pressure Profile of the G.E. Large Scale 4 Stage Rig (Ref. 5)

Design of Second-Generation Controlled Diffusion Airfoils

The previous sections have shown that the elements of the Integrated Core/Endwall aerodynamic model represent the physics of the endwall and core flowfields and their interaction with one another. The design philosopny of the first-generation Controlled Diffusion Airfoils is to apply high diffusion in the forward section of the airfoil chord where the boundary layer is thin and decrease the rate of diffusion aft according to the boundary layer health to prevent separation. This provided a decided benefit over previous standard airfoil series most of which had 10-15% of their chord separated. The same philosophy was extended from the core into the endwall region with only general recognition of the different nature of its flowfield.

The Integrated Core/Endwall model used in the analysis mode showed that the endwall blading of the first-generation CDA design, which had demonstrated 1980's state-of-the-art spanwise average efficiency, was at stalled incidence with severely separated boundary layers. As illustrated in Figure 13, the wall sections were analyzed to have excessive suction surface leading edge overspeed and resultant early separation compared to typical core sections. This separation occurred at both walls despite leading and trailing edge overcambers developed through years of testing and based on empirical data and simplified wall boundary layer modeling. It is also doubtful that the core blading of this design was operating at full capacity due to the change in the radial flowfield caused by the stalled endwall, although empirical blockage factors derived from test checkouts could account for much of it in this highly developed compressor. However, design studies conducted with the Integrated Core/Endwall Model revealed several blade angle and shape changes to improve endwall and overall performance. Model results for one representative endwall section are presented in Figure 14 to illustrate the benefits of endwall geometry changes. The most influential change was to match leading edge blade angle in the endwall region to prevent the suction surface overspeed.

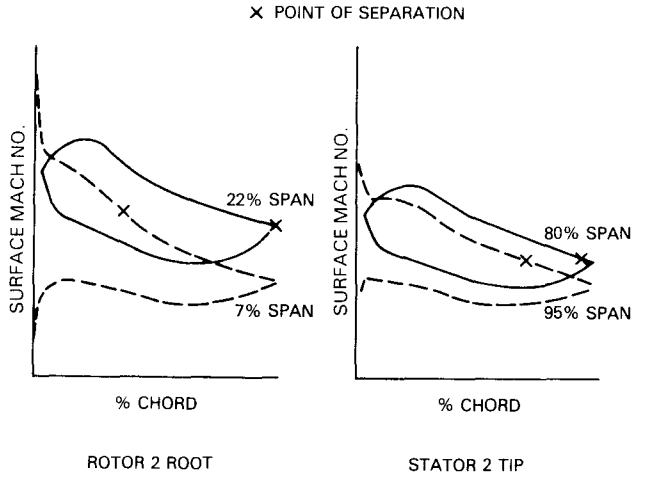

Fig. 13 Analysis of the 1st Generation CDA Baseline Design with the Integrated Core/Endwall Model Showed Severely Separated Wall Sections and Unseparated Core Sections

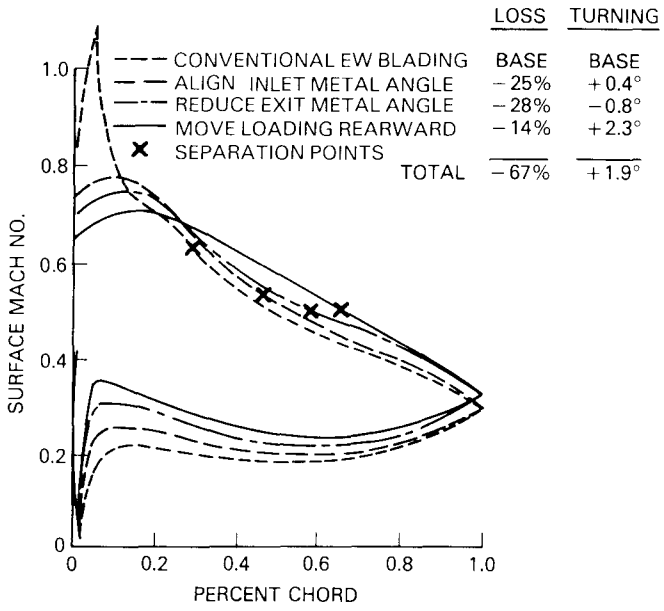

Fig. 14 2nd Generation CDA Endwall Geometry Changes Were Predicted to Produce Significant Improvements in Loss and Turning by Reducing Separation of 1st Generation CDA's

The aerodynamic model predicted that aligning the leading-edge metal angle would delay boundary layer separation 15% further aft on the blade chord and result in a 25% predicted reduction in loss of this typical rotor root endwall section. The model indicated the reduction in loss and a 0.4 degree increase in turning were derived by eliminating suction surface overspeed and rapid recompression, as shown in Figure 14, producing a healthier boundary layer.

The increase in turning and reduction in loss by aligning leading-edge incidence leads to the prospect of reducing work in the endwall sections. Trailing-edge metal angles can be reduced while still meeting the original design pressure ratio because of the more efficient sections. Studies showed that reducing the camber to reduce exit air angle only 0.8 degree resulted in a 28% reduction in total pressure loss cumulative with the leading-edge alignment benefit.

One of the major objectives of the second-generation CDA design was to exploit the potential of CDA section shape in improving endwall performance. Analysis showed that aft loading of the endwall sections by increasing the camber rate of the rear while reducing that of the front part of the airfoil chord resulted in a further 14% reduction in loss, 5% movement aft of the separation point, and a 2.3 degree increase in section turning.

The improvement in separation point and loss by moving diffusion aft was beneficial due to the high degree of separation in the endwall region. Core airfoil sections with 10 to 15% of their chord separated can be made unseparated by moving diffusion forward, but an endwall section with 30% or more of its chord separated cannot sustain enough front loading to eliminate separation. In this environment, the amount of separation was predicted to be reduced by unloading the front part of the airfoil resulting in a net predicted benefit in loss and turning. Since the benefit of the aft loading concept depended on the degree of separation, it was applied after employing the improved incidence and reduced work and was still predicted to improve loss and turning.

The cumulative total benefits of these three endwall geometry innovations tabulated in Figure 14 is a 67% predicted reduction in loss and 1.9 degree increase in turning for this typical section near the inner endwall. The amount of recambering of leading and trailing-edge angles and the section shape modifications varied depending on the airfoil row and spanwise position, due to the differing friction vortex strengths and extents of each section location. The mass-flow averaged, full-span, overall three-stage benefit of these endwall geometries when combined with the integrated core design was predicted to be approximately 1% in efficiency at 1.85 pressure ratio. The reduction in required work in the endwalls and the more efficient endwall sections also reduced aerodynamic loading in the endwalls, potentially improving surge margin. The more stable state of the boundary layer on these endwall sections should delay their aerodynamic breakdown as often occurs when the compressor is throttled up the speedline. Analysis of the improved endwall sections showed a 0.15 average reduction in diffusion factor and a reduced sensitivity to stalling incidence equivalent to 6% surge margin.

It is interesting to note that Wisler (Ref. 5) showed similar endwall geometry trends for improved performance based on low speed model testing. His geometry modifications were derived from direct analysis of test results, however, rather than a flow field model, and were applied differently. In Wisler's work, geometry twist gradients were applied only to stators in response to their separated pressure distributions, and aft-loaded sections were concluded to be beneficial only at rotor tips due to the tip leakage effect on surface pressure distribution; both concepts were found to be beneficial at all wall sections in the CDA-II studies discussed here.

A sample second-generation CDA stator stacked airfoil view from this rig design is presented in Figure 15. Note the impression of a twisted closed endwall given by the leading-edge alignment and reduction in work of the endwall sections. Although this CDA-II design is derived from a significantly more sophisticated model and analysis than previous designs, it is still partially empirical: a simplified approach to a very complex problem. In short, it is in need of test substantiation and development under realistic engine conditions.

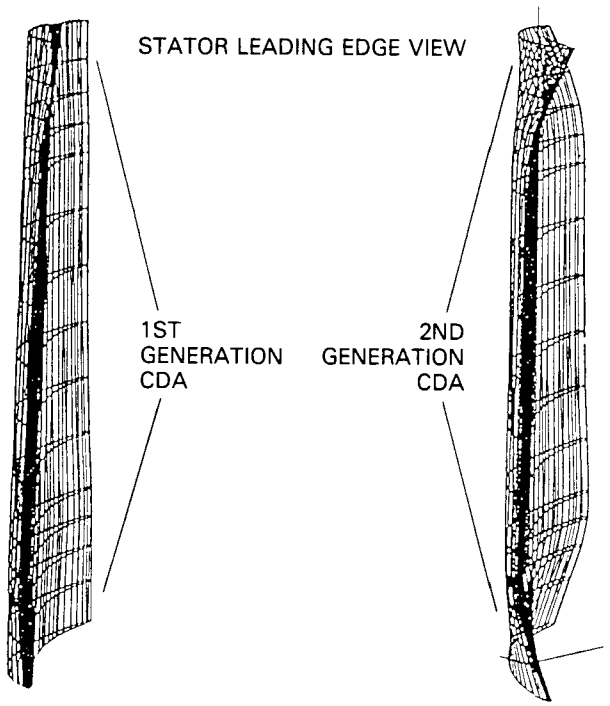

Fig. 15 The Radially Stacked Sections of the 2nd Generation CDA Design Reveal Significantly More Skewing of Metal Angle in the Endwall Region Compared to 1st Generation CDA's

HIGH MACH NUMBER MULTISTAGE RIG DEMONSTRATION OF SECOND-GENERATION CDA BENEFITS

Comparative First-Generation CDA Baseline Tests

The final objectives in the development of new technology is the demonstration of its benefits and its rapid assimilation into production engines. These objectives were met for the second-generation CDA geometry by demonstrating its performance in a high Mach number multistage rig test back-to-back with a first-generation CDA baseline. The closed circuit

compressor test facility (Figure 16) was designed specifically for this purpose by providing the capability to test full size engine hardware at engine levels of Mach number and Reynolds number. In this modern facility a heat exchanger is utilized to control rig inlet temperature while inlet pressure is boosted by an outside pressure source to vary Reynolds number. The 2250 horsepower motor permits testing in the size range of engine compressors using three stages to establish the multistage effects, but maintains a sizable cost advantage over testing of the full compressor.

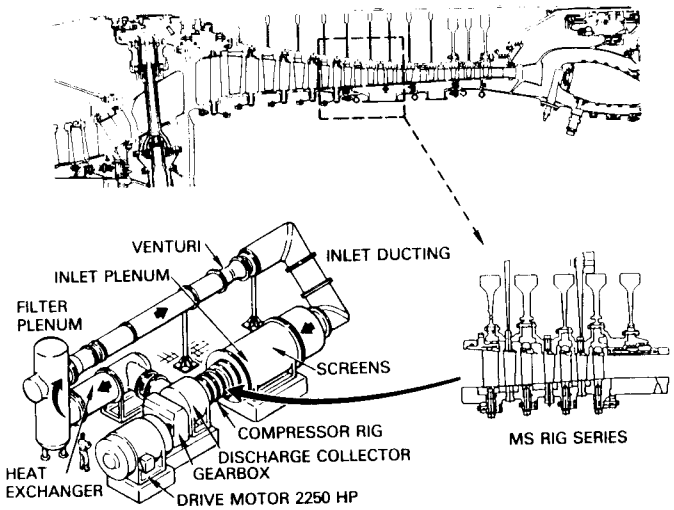

Fig. 16 Middle Stages of a Modern, Commercial HPC Were Duplicated and Tested at Engine Size, Reynolds Number, and Mach Number in a Modern, Closed Loop Facility to Establish a Realistic Baseline

The middle three stages of the PW2037 commercial engine high-pressure compressor were duplicated in exacting aerodynamic detail, as shown in Figure 16, to establish a realistic modern baseline for the development of second-generation Controlled Diffusion Airfoils. This rig has adjustable rotor and stator capability for aero development, but it has maintained the airfoil, flowpath, tip clearance and cavity dimensions of the original engine stages. A comparison of the closed loop baseline rig test characteristics with those of the equivalent PW2037 stages taken from an engine development high compressor test is presented in Figure 17.

The middle-stage group was tested with an inlet screen and inlet preswirl vanes to duplicate inlet boundary conditions from the engine. The close agreement of pressure and efficiency characteristic shapes attests to the care taken to duplicate engine geometry and operating environment. This middle-stage group rig is, therefore, a viable baseline for assessing the benefits of the second-generation Controlled Diffusion Airfoils.

High Mach Number Rig Testing of Second-Generation CDA Benefits

The test evaluation of second-generation Controlled Diffusion Airfoils at engine operating conditions in the high Mach number three-stage rig was both a performance success and a verification of

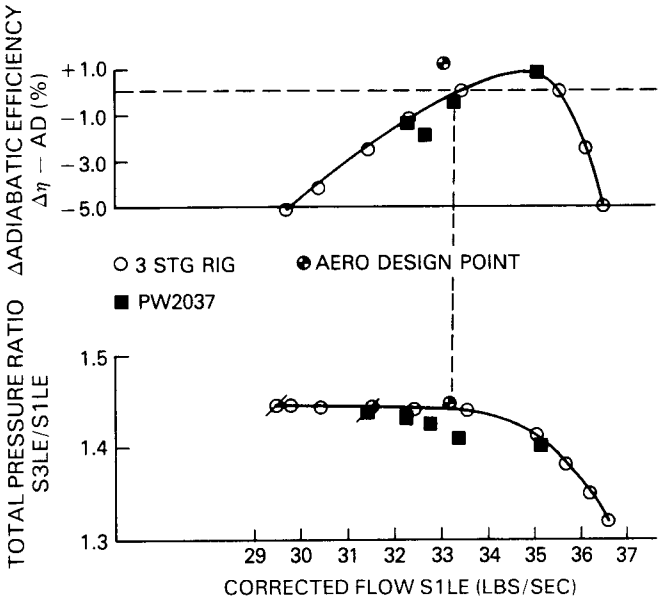

Fig. 17 Overall Characteristics of the Commercial Engine HPC Middle Stages Tested in the Closed Circuit Test Facility Matched Interstage Instrumentation Results from Full Rig Testing

the design-development system used. The as-designed CDA-II geometry produced a 1.5% increase in operating line efficiency and 8% increased surge margin relative to the CDA-I baseline as shown in the compressor map of Figure 18. The CDA-II speed line was notably more vertical than that of the baseline indicating that the endwalls were less stalled and able to sustain higher loading with less loss. The goal of matching the combined core and endwall at peak performance on the operating line was achieved; this resulted in a 1.5% efficiency gain on the operating line, where it will have the greatest impact on engine performance. A subsequent test in this rig revealed that efficiency and surge margin gains were substantially retained when the small flow deficit of the CDA-II in Figure 18 was eliminated by adding camber to the endwall region. This improvement has been designed into future models of commercial engines.

Although the performance improvements produced in High Mach Number Rig testing are of great value to the engines which can immediately absorb them, the feedback of data into the design-development system is of equal importance to future engines. Comparison of Mach number derived from airfoil surface static pressure measurements in Figure 19 provides a direct comparison of the modeled aerodynamics to test.

Predicted vane suction and pressure surface Mach numbers are reasonably good matches of the test shape and excellent matches of the overall diffusion at the inner wall, midspan and outer wall sections. Predicted midspan Mach number distribution is nearly identical to the test and confirms the design intent of eliminating separation by diffusing smoothly to the trailing-edge. The wall section predicted Mach number shapes are not as perfect matches of test as at midspan, but follow shape reasonably well and match overall diffusion at the predicted separation

point. A closer match of shape would be possible as previously discussed, if the viscous solution were recycled through the potential field calculation and iterated to a final solution. The fact that the overall performance of the CDA-II geometry designed with this model was successful suggests that this procedure is a reasonable basis for design.

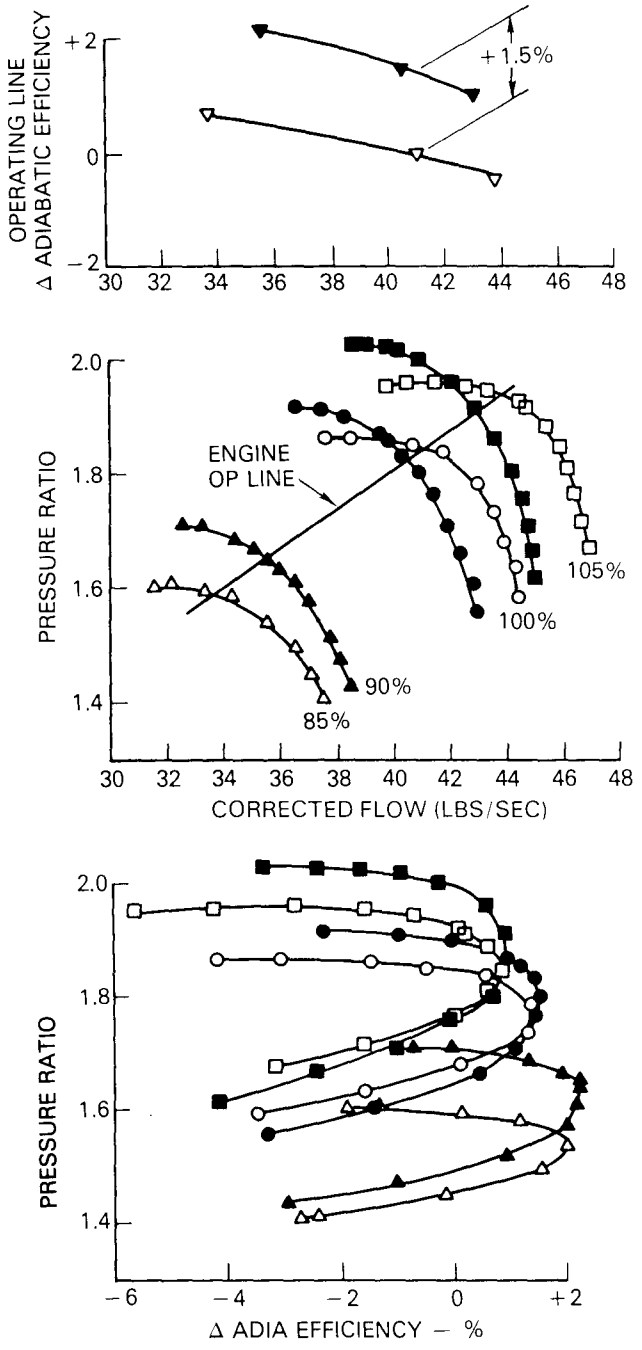

1ST GEN CDA BASE − OPEN SYMBOLS
2ND GEN CDA − SOLID SYMBOLS

Fig. 18 2nd Generation Controlled Diffusion Airfoils Increased Operating Line Efficiency by 1.5% with 8% Increased Surge Margin

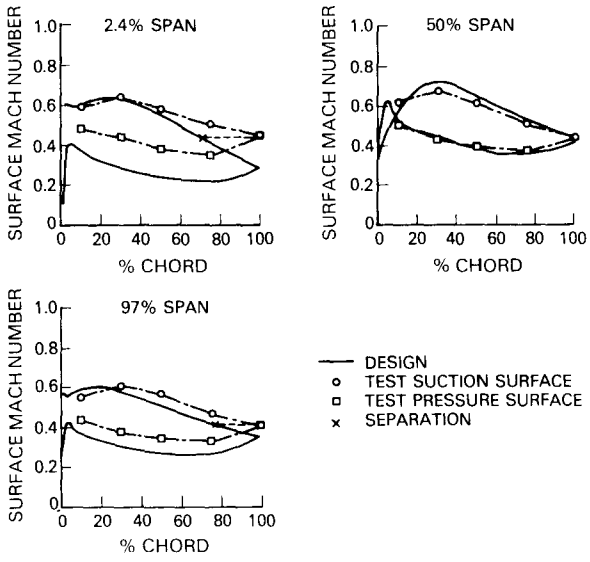

Fig. 19 High Mach Number, 3 Stage Test Airfoil Surface Static Pressure Measurements Match 2nd Generation Airfoil Design Intent

CONCLUDING REMARKS

The successful demonstration of second-generation CDA geometry at engine conditions has shown that the extension of CDA technology to the endwalls using an Integrated Core/Endwall aerodynamic model is an effective approach to developing new technology in multistage compressors. The 1.5% increase in operating line efficiency and 8% gain in surge margin confirms the overall design-development system of cascade, low and high Mach number rigs which supported this design model. These significant performance gains represent a new plateau of technology which must be exploited for maximum advantage to forthcoming engine multistage compressors. The improved surge margin of 8% is a 30% increase in surge-free operating capability, which can be used to push to higher lift/drag airfoils resulting in either fewer airfoils or greater pressure ratio per stage. Employing three-dimensional Euler multigrid/Navier Stokes improved flowfield definitions translated from fan experience into multistages, these high lift/drag principles can be transformed into the compact, high performance compressors needed for future high thrust/weight fuel efficient engines. These future generations of Controlled Diffusion Airfoils have the potential of improving multistage compressor efficiency an additional 1 to 2 percentage points with surge margins at least as good as present day compressors.

ACKNOWLEDGMENTS

The work described in this paper was accomplished by design, development, and test groups at Pratt & Whitney and the United Technologies Research Center. The success of this research is attributed to their spirit of cooperation and team-effort.

REFERENCES

1) Adkins, G.G. Jr., and Smith, L.H. Jr., "Spanwise Mixing in Axial-Flow Turbomachines," ASME Journal of Engineering for Power, Vol. 104, Jan. 1982

2) Hobbs, D.E., and Weingold, H.D., "Development of Controlled Diffusion Airfoils for Multistage Compressor Application," ASME 83-GT-211, 1983

3) Wagner, J.H., Dring, R.P., and Joslyn, H.D., "Inlet Boundary Layer Effects in an Axial Compressor Rotor: Part I -- Blade-to-Blade Effects," ASME 84-GT-84, June 1984

4) Wagner, J.H., Dring, R.P., and Joslyn, H.D., "Inlet Boundary Layer Effects in an Axial Compressor Rotor: Part II -- Throughflow Effects," ASME 84-GT-85, June 1984

5) Wisler, D.C., "Loss Reduction in Axial Flow Compressors Through Low-Speed Model Testing," ASME 84-GT-184, June 1984

6) Wisler, D.C., "Core Compressor Exit Stage Study," Vol. IV, NASA CR-159499, April 1981, and Vol. I, "Blading Design," NASA CR135391, Dec. 1977